

MICROCOPY

CHART

12

AD-A167 748

PREDICTION OF GUST LOADINGS AND ALLEVIATION AT TRANSONIC SPEEDS

by

David Nixon
and
Keh Lih Tzuoo

DTIC FILE COPY



DTIC
ELECTE
MAY 0 2 1986
S
D
E

**NIELSEN ENGINEERING
AND RESEARCH, INC.**

OFFICES: 510 CLYDE AVENUE / MOUNTAIN VIEW, CALIFORNIA 94043 / TELEPHONE (415) 968-9457

for public
distribution

86 5 1 001

CONF. NO. 16 12

PREDICTION OF GUST LOADINGS AND
ALLEVIATION AT TRANSONIC SPEEDS

by

David Nixon
and
Keh Lih Tzuoo

DTIC
SELECTE
MAY 02 1986
E

This document has been approved
for public release and unlimited
distribution is authorized.

NEAR TR-352

PREDICTION OF GUST LOADINGS AND
ALLEVIATION AT TRANSONIC SPEEDS

David Nixon
and
Keh Lih Tzuoo
NIELSEN ENGINEERING & RESEARCH, INC.
510 Clyde Avenue
Mountain View, CA 94043-2287

March 1986

Final Report for Period 9/20/83 - 7/20/85

APPROVED FOR PUBLIC RELEASE; DISTRIBUTION IS UNLIMITED

Prepared for

DAVID W. TAYLOR NAVAL SHIP RESEARCH AND DEVELOPMENT CENTER
Bethesda, MD 20084-5000

Accession For	
NIS 0001	<input checked="" type="checkbox"/>
DTIC TAB	<input type="checkbox"/>
Unannounced	<input type="checkbox"/>
Justification	
By _____	
Distribution/	
Availability Codes	
and/or	
Dist. Special	
A-1	

Unclassified

SECURITY CLASSIFICATION OF THIS PAGE

REPORT DOCUMENTATION PAGE

1. REPORT SECURITY CLASSIFICATION UNCLASSIFIED		1b. RESTRICTIVE MARKINGS	
2a. SECURITY CLASSIFICATION AUTHORITY		3. DISTRIBUTION/AVAILABILITY OF REPORT APPROVED FOR PUBLIC RELEASE; DISTRIBUTION UNLIMITED	
5. DECLASSIFICATION/DOWNGRADING SCHEDULE			
4. PERFORMING ORGANIZATION REPORT NUMBER(S) NEAR TR-352		5. MONITORING ORGANIZATION REPORT NUMBER(S) DTNSRDC/ASED-CR-01-86	
6a. NAME OF PERFORMING ORGANIZATION Nielsen Engineering & Research, Inc.	6b. OFFICE SYMBOL (if applicable)	7a. NAME OF MONITORING ORGANIZATION David W. Taylor Naval Ship Research and Development Center	
6c. ADDRESS (City, State, and ZIP Code) 510 Clyde Avenue Mountain View, CA 94043		7b. ADDRESS (City, State, and ZIP Code) Bethesda, MD 20084-5000	
8a. NAME OF FUNDING/SPONSORING ORGANIZATION Naval Air Systems Command	8b. OFFICE SYMBOL (if applicable) NAVAIR-310D	9. PROCUREMENT INSTRUMENT IDENTIFICATION NUMBER N00167-83-C-0114	
8c. ADDRESS (City, State, and ZIP Code) Washington, DC 20361		10. SOURCE OF FUNDING NUMBERS	
		PROGRAM ELEMENT NO	PROJECT NO
		TASK NO.	WORK UNIT ACCESSION NO
11. TITLE (Include Security Classification) PREDICTION OF GUST LOADINGS AND ALLEVIATION AT TRANSONIC SPEEDS			
12. PERSONAL AUTHOR(S) David Nixon and Keh Lih Tzuoo			
13a. TYPE OF REPORT Final Report	13b. TIME COVERED FROM 9/20/83 to 7/20/85	14. DATE OF REPORT (Year, Month, Day) 1986, March	15. PAGE COUNT 36
16. SUPPLEMENTARY NOTATION			
17. COSATI CODES		18. SUBJECT TERMS (Continue on reverse if necessary and identify by block number)	
FIELD	GROUP	SUB-GROUP	
20	04	→ Transonic Flow; Unsteady Aerodynamics, ←	
20	11		
19. ABSTRACT (Continue on reverse if necessary and identify by block number) The transonic indicial theory is used to predict the effect of a gust on an airfoil at transonic speeds. The effect of operating two control surfaces is also modeled by the indicial method. The transonic indicial method is linear in a strained coordinate system and superposition can be used. This allows the effects of an arbitrary gust and control surface deflection to be modeled simply if the indicial responses for the gust and each control surface are known. The computation time is small and, therefore an optimization technique can be used to determine the best control surface deflections to alleviate the gust loading.			
20. DISTRIBUTION/AVAILABILITY OF ABSTRACT <input type="checkbox"/> UNCLASSIFIED/UNLIMITED <input checked="" type="checkbox"/> SAME AS RPT. <input type="checkbox"/> OTIC USERS		21. ABSTRACT SECURITY CLASSIFICATION UNCLASSIFIED	
22a. NAME OF RESPONSIBLE INDIVIDUAL David Nixon		22b. TELEPHONE (Include Area Code) (415) 968-9457	22c. OFFICE SYMBOL

TABLE OF CONTENTS

LIST OF FIGURES.....	iii
ABSTRACT.....	v
Introduction.....	1
Basic Equations.....	4
Piston Theory Limit for a Step Change in Normal Velocity.....	6
The Transonic Indicial Method.....	8
Curve Fits of Indicial Data.....	11
Model of Gust Alleviation.....	13
Control Optimization.....	15
Gust Response.....	16
Results.....	18
Possible Extensions of Work.....	20
Conclusions.....	21
REFERENCES.....	23-24
FIGURES.....	25-36

LIST OF FIGURES

- Figure 1. Steady state pressure distribution for a NACA 0012 airfoil.
- Figure 2. Test case comparison between present method and XTRANL for a NACA 0012 airfoil at $M_\infty = 0.601$ and $\alpha_m = 2.89$ degrees.
- Figure 3. C_L comparison between gust with and without control surface deflection alleviation for a NACA 0012 airfoil at $M_\infty = 0.601$ and $\alpha_m = 2.89$ degrees.
- Figure 4. C_M comparison between gust with and without control surface deflection alleviation for a NACA 0012 airfoil at $M_\infty = 0.601$ and $\alpha_m = 2.89$ degrees.
- Figure 5. Steady state pressure distribution for a NACA 64A006 airfoil.
- Figure 6. Test case comparison between present method and XTRANL code for a NACA 64A006 airfoil at $M_\infty = 0.825$ and $\alpha_m = 1$ degree.
- Figure 7. C_L comparison between gust with and without control surface deflection alleviation for a NACA 64A006 airfoil at $M_\infty = 0.825$ and $\alpha_m = 1$ degree.
- Figure 8. C_M comparison between gust with and without control surface deflection alleviation for a NACA 64A006 airfoil at $M_\infty = 0.825$ and $\alpha_m = 1$ degree.
- Figure 9. Steady state pressure distribution for an MBB-A3 airfoil.

Figures (cont.)

Figure 10. Test case comparison between present method and XTRANL code for an MBB-A3 airfoil at $M_\infty = 0.7$ and $\alpha_m = 1$ degree.

Figure 11. C_L comparison between gust with and without control surface deflection alleviation for an MBB-A3 airfoil at $M_\infty = 0.7$ and $\alpha_m = 1.5$ degrees.

Figure 12. C_M comparison between gust with and without control surface deflection alleviation for an MBB-A3 airfoil at $M_\infty = 0.7$ and $\alpha_m = 1.5$ degrees.

ABSTRACT

The transonic indicial theory is used to predict the effect of a gust on an airfoil at transonic speeds. The effect of operating two control surfaces is also modeled by the indicial method. The transonic indicial method is linear in a strained coordinate system and superposition can be used. This allows the effects of an arbitrary gust and control surface deflection to be modeled simply if the indicial responses for the gust and each control surface are known. The computation time is small and, therefore, an optimization technique can be used to determine the best control surface deflections to alleviate the gust loading.

1. Introduction

One of the more pressing problems in designing a modern aircraft that flies at transonic speeds is the prediction of the gust response. A knowledge of the loading induced by a gust is necessary for the aerodynamicist to predict its effect on wing performance and for the structural engineer to design a sufficiently strong structure and, perhaps, to implement active controls to reduce the load. At present, the capability to accurately predict gust loading at transonic speeds does not exist. It is this problem that is addressed in the present work.

Aeroelastic calculations are frequently performed using linear theory for both the structure and the aerodynamic loads. This leads to a relatively simple means of estimating flutter speeds, since linearity permits the use of the principle of superposition. Linear aerodynamic theory is really only applicable to the subsonic or supersonic speed regimes; the transonic regime is essentially nonlinear. This nonlinearity is associated with shock-wave formation, often accompanied in unsteady flow with complex shock oscillations. It is essential, therefore, to include the nonlinearities in some way in order to predict transonic flow phenomena. For the most general case, this requires the development of a three-dimensional transonic flow computer code for predicting unsteady effects including viscous interactions between any shock waves that form and the boundary layer on the surface of the structure. Although progress is being made toward the development of such a code,¹ this is only half the problem, since the aerodynamic loads must interact with a dynamic structural model in order to predict aeroelastic phenomena. Accomplishing this interaction with a large and complex unsteady flow transonic code is not a trivial matter, and major advances in computer size and speed will be necessary before calculations of this sort can be routinely used in either the analysis or the design of aircraft.

A further problem is that conventional gust analysis may impose an upwash of finite length into the free stream. If this upwash is completely arbitrary, the flow is unlikely to be irrotational throughout the gust. Since all of the available transonic solution methods are based on potential (irrotational) theory,^{1,2} this presents difficulties in easily developing a gust load prediction method.

If the gust loading can be predicted, it is possible that some means to reduce the loading can be developed, perhaps by the deflection of a control surface. Also, due to the coupling of the mean steady and unsteady loading in a nonlinear transonic theory, certain wings may be more sensitive than others to gusts.

The work reported is concerned with a preliminary study of transonic gust loading and its alleviation. To retain simplicity at this stage, only two-dimensional problems are considered.

In recent years the numerical simulation of steady transonic flow has reached a fairly advanced stage. For example, the two-dimensional codes based on the original algorithm of Murman and Cole³ are frequently used in the aircraft industry. Three-dimensional variations of these codes for finite wings and wing-body combinations are also available, such as the codes of Bailey and Ballhaus⁴ (transonic small disturbance) and Jameson and Caughey⁵ (full potential). While these codes have certain deficiencies, they have been extremely useful in aircraft design.

The state of the art regarding codes for unsteady flow is not as advanced as that for steady transonic flow. The direct integration method of Ballhaus and Goorjian² for low frequency two-dimensional flows is a reliable tool. There have been several extensions of this theory to high frequency flows, notably by Rizzetta and Chin⁶ and by the XTRANL code developed by

Whitlow⁷ at NASA Langley Research Center. Also, several preliminary attempts have been made to extend these two-dimensional algorithms to three-dimensional flow. Perhaps the most mature of these is the method developed by Rizzetta and Borland¹. However, this three-dimensional code is very expensive to run on a computer at present. All of these methods are based on potential theory.

In view of the computational expense in obtaining a transonic flow calculation, it is desirable to increase the usefulness of one calculation; to this end, the transonic indicial theory^{8,9} can be used. The indicial theory depends on the validity of the principle of superposition. Such a method is not valid at transonic speeds because of the necessary nonlinearity of the governing equations that represent the flow with moving shock waves. In certain circumstances, however, unsteady transonic flow quantities can be represented by a linearized equation while the shock motion is still taken into account. Nixon⁹ has shown that the transonic indicial method of Ballhaus and Goorjian⁸ properly accounts for shock motion effects, if only integrated properties such as airfoil lift and moment coefficients are considered. The shock motion need not be explicitly included since it already appears in the calculation of the indicial response. A similar result applies for control-surface hinge moments if the shock does not oscillate across the hinge. When the shock oscillates across the hinge, the strained-coordinate method of Nixon⁹ can be used to treat the shock motion. An application of the indicial approach is given in Reference 10.

In the indicial theory of Nixon,⁹ the nonlinear problem is decoupled into two linear problems in which superposition is valid. Since superposition can be used, it is also possible to superpose the effects of various elements in an unsteady flow,

such as flap movements or changes in angle of attack, provided the indicial response of each component in isolation is known. The capability to superpose is one of the most powerful features of the indicial method.

In connection with reducing loading at transonic speeds, it should be noted that a preliminary attempt was made by Ballhaus et al.¹¹ to study the effects of moving leading and trailing edge flaps on the loads on an airfoil.

The present work combines the methods of Kerlick and Nixon¹⁰ and the XTRANL code to give the gust response of an airfoil. In addition, the effect of two control surfaces on the flow is included in the model. These methods are augmented by the use of the optimization code CONMIN in determining the control surface deflections to minimize the additional loading due to the gust. Because the computer time required by the indicial theory is greatly reduced, the optimization code is economical to use.

2. Basic Equations

The model equation used in the present work is the unsteady transonic small disturbance equation

$$\phi_{xx} + \phi_{yy} - 2 \frac{M_{\infty} c^2}{U_{\infty}} \phi_{xt} - M_{\infty}^2 \frac{c^2}{U_{\infty}^2} \phi_{tt} = k \phi_x \phi_{xx} \quad (1)$$

where $\phi(x,y,t)$ is the perturbation velocity potential; x and y are cartesian coordinates scaled by the airfoil chord, c ; and U_{∞} is the free-stream velocity. The constant k is given by

$$k = [3 + (\gamma - 2) M_{\infty}^2] M_{\infty}^2 \quad (2)$$

where γ is the ratio of specific heats.

The appropriate boundary conditions are that the flow behaves like outgoing waves as

$$x^2 + y^2 \rightarrow \infty \quad (3)$$

and that the flow is tangent to the airfoil. This tangency condition is satisfied in a thin airfoil sense by ensuring that

$$\phi_y(x, \pm 0, t) = \frac{\partial y_s(x, \pm 0, t)}{\partial x} + \frac{c}{U_\infty} \frac{\partial y_s(x, \pm 0, t)}{\partial t} \quad (4)$$

where $y = y_s(x, \pm 0, t)$ denotes the ordinate of the airfoil boundary at station x and time t . The problem is completed by ensuring that the wake, represented by $y = 0$, carries no load. Thus, on the wake (and at the trailing edge of the airfoil)

$$C_p(x, +0, t) = C_p(x, -0, t) \quad (5)$$

where $C_p(x, y, t)$ is the pressure coefficient given by

$$C_p(x, y, t) = -2 \left(\phi_x + \frac{c}{U_\infty} \phi_t \right) \quad (6)$$

The boundary condition, Equation (4), can be written as

$$\begin{aligned} \phi_y(x, \pm 0, t) = & \frac{\partial \bar{y}_s(x, \pm 0)}{\partial x} + \frac{\partial \hat{y}_s(x, \pm 0, t)}{\partial x} \\ & + \frac{c}{U_\infty} \frac{\partial \hat{y}_s(x, \pm 0, t)}{\partial t} \end{aligned} \quad (7)$$

where \bar{y}_s and \hat{y}_s represent the steady and unsteady components, respectively. For a control surface deflected at $\beta(t)$, $\hat{y}_s(x, \pm 0, t)$ is given by

$$\hat{y}_s(x, \pm 0, t) = -\beta(t) (x - x_h) H(x - x_h) \quad (8)$$

where x_h is the location of the control surface hinge and $H()$ is the step function.

In the present analysis, a semi-infinite gust is modeled by the boundary condition

$$\phi_y(x, \pm 0, t) = \frac{\partial \bar{y}_s(x, \pm 0)}{\partial x} + v_G(x, t) \quad (9)$$

Thus,

$$\begin{aligned} v_G(x, t) &= |v_G|, & x < U_\infty(t - t_0) \\ &= 0, & x > U_\infty(t - t_0) \end{aligned} \quad (10)$$

where $|v_G|$ is the magnitude of the gust velocity; the gust starts at $t = t_0$ and travels with the free-stream velocity U_∞ . The gust model is similar to that of McCroskey and Goorjian.¹²

3. Piston Theory Limit for a Step Change in Normal Velocity

In the early phase of subsonic and supersonic flutter analysis, great use was made of the piston theory limit. Briefly, the supposition was that if the airfoil oscillated at very high frequencies, the velocity of the airfoil surface was an order of magnitude greater than the streamwise velocity. As a consequence, the linearized version of Equation (1) becomes

$$\phi_{yy} = M_\infty^2 \frac{c^2}{U_\infty^2} \phi_{tt} \quad (11)$$

The solution is

$$\phi = f\left(y \mp \frac{U_\infty c}{M_\infty} t\right) \quad (12)$$

For $y > 0$, the positive sign is taken; for $y < 0$, the negative sign is used. This is to ensure outgoing waves. The pressure coefficient in the approximation of Equation (11) is given by

$$C_p(x, \pm y, t) = -2 \frac{c}{U_\infty} \phi_t(x, \pm y, t) \quad (13)$$

From Equation (12),

$$\phi_y(x, y, t) = f' \left(y \mp \frac{U_\infty c}{M_\infty} t \right) \quad (14)$$

For a step change in the normal velocity component of $-\alpha$, Equation (14) gives

$$f'(0) = -\alpha \quad (15)$$

Combining Equations (13) and (15) gives the result

$$C_p(x, \pm 0, 0) = \mp \frac{2\alpha}{M_\infty} \quad (16)$$

This is the initial pressure coefficient experienced by the airfoil due to a step change in angle of attack.

In the transonic equation, Equation (1), there is no mechanism to invalidate the basic premise of piston theory; namely, that streamwise velocities are small relative to the normal velocity. Hence, Equation (16) is valid for transonic flow. Furthermore, since streamwise velocities contain the shock mechanism for Equation (1), the initial movement of shock does not enter Equation (11). Therefore, it is assumed that the shock movement does not start with the discontinuity that characterizes the pressure coefficient.

4. The Transonic Indicial Method

In linear models of subsonic or supersonic flow, an alternative to expanding the governing equation in a Fourier series is to use an indicial function. An indicial function analysis depends on the governing equation being linear, which is not the case for transonic flow. However, if the amplitude of motion is small and if shock waves are not generated or destroyed during the motion, a linear equation similar to that used in subsonic flow can be derived to model the unsteady motion. This is the basis for the work of Kerlick and Nixon.¹⁰ The following briefly outlines their work:

Consider the change in the pressure coefficient $C_p(x, y, t)$ due to an infinitesimal change in some parameter $\epsilon(\tau)$ at some time τ . If the pressure distribution varies continuously with ϵ , a Taylor's series expansion gives

$$\Delta C_p(x, y, t) = C_{p_\epsilon}(x, y, t, \tau) \frac{d\epsilon(\tau)}{d\tau} \Delta\tau + \text{higher-order terms} \quad (17)$$

where t is the time and $C_{p_\epsilon}(x, y, t, \tau)$ is the rate of change of $C_p(x, y, t)$ with ϵ at some time τ ; $\Delta C_p(x, y, t)$ is the change in pressure distribution. Neglecting the higher order terms, the total effect of all such steps up until time t is then

$$\Delta C_p(x, y, t) = \epsilon(0)C_{p_\epsilon}(x, y, t, 0) + \int_0^t C_{p_\epsilon}(x, y, t, \tau) \frac{d\epsilon(\tau)}{d\tau} d\tau \quad (18)$$

If it can be assumed that the behavior of C_p with ϵ is linear, $C_{p_\epsilon}(x, y, t, \tau)$ can be represented by its value at $\tau = 0$, provided that the time t is taken relative to τ . Thus,

$$C_{p_\epsilon}(x, y, t, \tau) = C_{p_\epsilon}(x, y, t - \tau, 0) \quad (19)$$

Equation (18) then becomes

$$\Delta C_p(x, y, t) = \epsilon(0) C_{p_\epsilon}(x, y, t, 0) + \int_0^t C_{p_\epsilon}(x, y, t-\tau, 0) \frac{d\epsilon(\tau)}{d\tau} d\tau \quad (20)$$

By a simple change of variable, Equation (20) can then be written as

$$\Delta C_p(x, y, t) = \epsilon(0) C_{p_\epsilon}(x, y, t) + \int_0^t C_{p_\epsilon}(x, y, \tau) \frac{d\epsilon(t-\tau)}{d\tau} d\tau \quad (21)$$

where the functional form of $C_{p_\epsilon}(x, y, t, 0)$ has been contracted to $C_{p_\epsilon}(x, y, t)$ for convenience in presentation. Equation (21) is the form of a typical relation in the indicial method. It is assumed that $C_{p_\epsilon}(x, y, t)$ can be obtained either analytically or numerically. In the foregoing analysis, it has been assumed that the variation of $C_p(x, y, t)$ with ϵ is linear. For continuous flows governed by a nonlinear equation, this assumption may well be adequate for small values of ϵ . However, as pointed out by Nixon,⁹ if there are shock waves that move during the motion, the assumption of linear variation is totally inadequate in the region bounded by the extremities of the shock motion. This is because the pressures in this region can jump from a pre-shock value to a post-shock value, or vice versa, as the shock traverses this region. This difficulty can be overcome by the use of a strained coordinate system in which the shock remains at the same location.

Let the strained coordinate system be given by (x', y, t) , which is related to the physical coordinate system (x, y, t) by

$$x = x' + \delta x_s(t) x_1(x') \quad (22)$$

where $\delta x_s(t)$ is the change in shock location at some time t , and $x_1(x')$ is a known straining function. In Equation (22), it is assumed that the shock waves are normal to the free stream.

Following the ideas of Nixon,⁹ $C_p(x,y,t)$ is given by

$$C_p(x,y,t) = C_{p_0}(x',y) [1 - \delta x_s(t) x_{1_{x'}}(x')] + C_{p_1}(x',y,t) \quad (23)$$

where $C_{p_0}(x',y)$ and $C_{p_1}(x',y,t)$ are the values for the mean steady state pressure and the unsteady perturbation, respectively. The coordinates x' and x are related by Equation (22).

In Equation (23), $\delta x_s(t)$ and $C_{p_1}(x',y,t)$ are linearly dependent on the parameter $\epsilon(\tau)$ and, therefore, can be treated by the indicial method. The nonlinear effect appears implicitly through the transformation from the strained coordinates to the physical coordinates. Thus,

$$\delta x_s(t) = \delta x_{s_\epsilon}(t) \epsilon(0) + \int_0^t \delta x_{s_\epsilon}(\tau) \frac{d\epsilon(t-\tau)}{d\tau} d\tau \quad (24)$$

$$C_{p_1}(x',y,t) = C_{p_\epsilon}(x',y,t) \epsilon(0) + \int_0^t C_{p_\epsilon}(x',y,\tau) \frac{d\epsilon(t-\tau)}{d\tau} d\tau \quad (25)$$

where $\delta x_{s_\epsilon}(t)$ and $C_{p_\epsilon}(x',y,t)$ are the indicial responses of $\delta x_s(t)$ and $C_{p_1}(x',y,t)$, respectively. The indicial responses can be obtained by computing the transient behavior of the shock motion and the pressure coefficient due to a step change in ϵ . This transonic calculation must only be performed once for a range of functions $\epsilon(\tau)$.

Equations (24) and (25) are linear; thus, the principle of superposition can be used. In the present work, the unsteady flows due to a gust and two control devices are superposed. In this case,

$$\delta x_s(t) = \sum_{i=1}^3 \left\{ \delta x_{s_{\epsilon_i}}(t) \epsilon_i(0) + \int_0^t \delta x_{s_{\epsilon_i}}(\tau) \frac{d\epsilon_i(t-\tau)}{d\tau} d\tau \right\} \quad (26)$$

$$C_{p_1}(x', y, t) = \sum_{i=1}^3 \left\{ C_{p_{\epsilon_i}}(x', y, t) \epsilon_i(0) + \int_0^t C_{p_{\epsilon_i}}(x', y, \tau) \frac{d\epsilon_i(t-\tau)}{d\tau} d\tau \right\} \quad (27)$$

where the subscript i denotes a flow perturbation due to the i th device (either controls or the gust).

5. Curve Fits of Indicinal Data

It is considerably helpful in the numerical evaluations of Equations (26) and (27) if the indicinal responses can be represented by analytic functions since the convolution integrals can then be evaluated analytically. In the present work, the indicinal responses for both the pressure coefficient and the shock movement are approximated as

$$f(x, t) = a + b \exp(-\alpha t) + c \exp(-\beta t) \quad (28)$$

where $f(x, t)$ is a general indicinal response and a , b , c , α , and β are functions of x , in general. The reason for including a second exponential term in Equation (28) is to allow for an inflection point on the indicinal response curve. At $t = 0$, $f(x, 0)$ is represented by its piston theory limit $f_p(x)$. Thus,

$$f_p(x) = a + b + c \quad (29)$$

As $t \rightarrow \infty$, $f(x, t)$ must approach its steady state value $f(x, \infty)$ corresponding to the step change in ϵ . Thus,

$$f(x, \infty) = a \quad (30)$$

Combining Equations (28), (29), and (30) gives

$$f(x, t) = f(x, \infty) [1 - \exp(-\alpha t)] + f_p(x) \exp(-\alpha t) \\ + c [\exp(-\beta t) - \exp(-\alpha t)] \quad (31)$$

Apart from the initial jump predicted by piston theory, the indicial response is a smooth curve. Consequently, $[f(x, t) - f_p(x)]/f(x, \infty)$ can be approximated by

$$[f(x, t) - f_p(x)]/f(x, \infty) = [1 - f_p(x)/f(x, \infty)] [1 - \exp(-\alpha t)] \\ + \frac{c}{f(x, \infty)} [\exp(-\beta t) - \exp(-\alpha t)] \quad (32)$$

The actual values of $f(x, t)$ are generated by numerical data. The coefficients c , α , and β are found by using Equation (32) in conjunction with the computer program CONMIN, which minimizes the objective function

$$[f(x, t) - f_p(x, 0)]/f(x, \infty) - [1 - f_p(x)/f(x, \infty)] [1 - \exp(-\alpha t)] \\ - c/f(x, \infty) [\exp(-\beta t) - \exp(-\alpha t)]$$

over the computed range of t . For the pressure coefficient

$$f_p(x) = \bar{p} + \frac{+2\alpha}{M_\infty} \quad (33)$$

and for the shock motion

$$f_p = 0 \quad (34)$$

The program for the curve fit was based on an early version provided by Dr. Samuel C. McIntosh of McIntosh Structural Dynamics, Inc.

6. Model of Gust Alleviation

A model problem was developed to test the applicability of the indicial method to model gust alleviation. The problem consists of a "top hat" gust that crosses the leading edge at time t_{10} and two control surfaces. For generality of computation, the sharp edge of the gust is replaced by a continuous variation similar to that of the control surfaces as given below. The characteristic times of the control surface are t_{10} , t_{11} , t_{12} , and t_{13} .

At $t = t_{20}$, the control surface moves according to the law

$$\alpha = \alpha_0 [1 - \cos \omega_{21}(t - t_{20})]/2, \quad t_{20} < t < t_{21} \quad (35)$$

where ω_{21} is given by

$$\omega_{21} = \pi/(t_{21} - t_{20}) \quad (36)$$

At time t_{21} the control stops. At time t_{22} , the control moves according to the law

$$\alpha = \alpha_0 [\cos \omega_{22}(t - t_{22}) + 1]/2, \quad t_{22} < t < t_{23} \quad (37)$$

where

$$\omega_{22} = \pi/(t_{23} - t_{22}) \quad (38)$$

The second control surface moves in an analogous manner on the first control.

The control motion described by Equation (35) has zero angular velocity at $t = t_{20}$ and t_{21} , which seems to be a realistic assumption. A similar behavior occurs at t_{22} and t_{23} .

In the indicial formulation, a typical quantity is given by

$$f(t) = f_{\epsilon}(t) \epsilon(0) + \int_0^t f_{\epsilon}(\tau) \frac{d\epsilon(t-\tau)}{d\tau} d\tau \quad (39)$$

where $f_{\epsilon}(t)$ is the indicial response. For the control laws described, $f(t)$ is given by

$$f(t) = \frac{\alpha_0}{2} \omega \int_{\hat{t}_0}^{\hat{t}_1} f_{\epsilon}(\tau) \sin \omega(t - \tau + t_0) d\tau \quad (40)$$

where the generic control law

$$\alpha = \alpha_0 [1 - \cos \omega(t - t_0)]/2 \quad (41)$$

is used.

If the control surface movement starts at t_0 and finishes at t_1 ,

$$\frac{d\epsilon(t-\tau)}{d\tau} = 0 \quad \text{for} \quad \begin{array}{l} t - \tau + t_0 < t_0 \\ t - \tau + t_0 > t_1 \end{array} \quad (42)$$

or, for a nonzero value of the integrand,

$$t + t_0 - t_1 < \tau < t \quad (43)$$

Also, for the general limits on the integral,

$$t_0 < \hat{t}_0; \hat{t}_1 < t \quad (44)$$

Hence, the limits are

$$\begin{aligned} \hat{t}_0 &= \max[t_0, t + t_0 - t_1] \\ \hat{t}_1 &= t \end{aligned} \quad (45)$$

7. Control Optimization

Calculations using the indicial response require very little computer time. Thus, it is economical to couple the gust response and the control model to an optimizer to determine the best control deflections and to minimize the objective function F , where

$$F = \Delta C_L^2 + \omega \Delta C_M^2 \quad (46)$$

There, ΔC_L and ΔC_M are the incremental lift and moment coefficients, and ω is a specified weighting function. The moments are about the quarter chord. The variables used in the optimization are the times t_{jk} ($j = 2, 3; k = 0, 1, 2, 3$) described in the previous section and the amplitudes of the control surface deflections. Constraints on t_{jk} are enforced; namely, that the control surface cannot operate until the gust has passed by 0.1 time units and that the finish time of a control deflection cannot occur before the start time of the deflection.

The objective of this exercise is to devise simple control systems to counter the gust. The computer code CONMIN is used for the optimization.

8. Gust Response

In linear subsonic flow, the gust response is a function only of the free-stream Mach number and the gust characteristics. In nonlinear transonic flow, the response is also a function of the steady flow over the airfoil and, hence, the airfoil geometry. This coupling manifests itself in two ways. First, the asymptotic lift of the wing due to a step in angle of attack, α , can be much greater than the classic value of $2\pi\alpha/\beta$, where

$$\beta = (1 - M_\infty^2)^{1/2}$$

Second, the characteristic time of the response, that is the transient behavior, is different from that in subsonic flow. For an airfoil to have a low gust response, the asymptotic lift increment of C_L due to the gust should be small. Also, the characteristic time should be large to allow for a control to operate.

For a gust alleviation device, the incremental lift, ΔC_L , should be large so that the control is effective; the characteristic time should be small so that the effect of the control occurs as early as possible.

In transonic flow there is a nonlinear coupling between the steady and unsteady flows that possibly could be used to some advantage. Consider that the unsteady lift coefficient C_L is represented as follows:

For a gust

$$C_L = \bar{C}_L \left[1 - e^{-\bar{c}(t + t_0)} \right] \quad (47)$$

where \bar{f}_∞ is the value of C_L as $t \rightarrow \infty$, \bar{c} is a constant, and the gust starts at $t = -t_0$.

For a control surface

$$C_L = f_\infty + (f_p - f_\infty) e^{-ct} \quad (48)$$

where f_∞ is the value of C_L at $t \rightarrow \infty$, and f_p is the value for piston theory at $t = 0$.

Let the control law be

$$\begin{aligned} \alpha &= \frac{\alpha_0}{2} (1 - \cos \omega t) & 0 < t < t_1 \\ \alpha &= \alpha_0 & t > t_1 \end{aligned} \quad (49)$$

and

$$\omega t_1 = \pi$$

Using Equations (47), (48), and (49) in the indicial equations of section 4 gives the total unsteady lift as

$$C_{L_T} = f_\infty \left\{ 1 + g + e^{-ct} \left[\frac{(1 + e^{\gamma\pi})(F - 1)}{2(1 + \gamma^2)} - g e^{-\bar{c}t_0} \right] \right\} \quad (50)$$

where $g = \bar{f}_\infty / f_\infty$

$$\gamma = c/\omega \quad (51)$$

and

$$F = f_p / f_\infty$$

For C_{L_T} to be zero for all $t > t_0$,

$$g = -1 \quad (52)$$

$$F = 1 + 2 \frac{g e^{-\bar{c}t_0} (1+\gamma^2)}{(1 + e^{\gamma\pi})}$$

or, using Equation (52),

$$F = 1 - \frac{2 e^{-\bar{c}t_0} (1+\gamma^2)}{(1 + e^{\gamma\pi})} \quad (53)$$

For linear subsonic flow at a fixed Mach number, f_p , f_∞ , and c are independent of airfoil section; ω is specified. Hence, there is no mechanism by which Equation (53) can be satisfied in general. However, for transonic flow the quantities f_∞ and c are dependent on airfoil geometry, and it is possible that a certain design of airfoil and control surface could satisfy Equation (52) leading to an effective gust alleviation device.

9. Results

The computer code XTRANL is used to compute the necessary indicial responses and to compute fully nonlinear cases for comparison.

In the following cases, the gust is of a "top hat" geometry, starting at $t = 0$ and ending at $t = 50$. There are two control surfaces, each of 10-percent chord extent. One control is at the leading edge, the other is at the trailing edge. In the test cases, the controls operate at the time shown in the following table. For the optimization cases, the gust amplitude is 1.5 degrees.

Table 1. Values of T_{rj}

r j	0	1	2	3
1	0.0	4.36×10^{-5}	50.0	$50 + 4.36 \times 10^{-5}$
2	0.0	22.0	60.0	82.0
3	0.0	22.0	60.0	82.0

Note: r = 1, Gust
r = 2, Trailing edge control
r = 3, Leading edge control

The steady pressure distribution around a NACA 0012 airfoil at $\alpha_m = 2.89$ degrees and $M_\infty = 0.601$ is shown in Figure 1. This is a subcritical example. In Figure 2, the prediction of the lift for this steady configuration is shown with a "top hat" gust with amplitude equivalent to 0.25 degrees and two control surfaces deflected at 0.25 degrees. The agreement with the direct result is quite good.

In Figures 3 and 4, the incremental lift and moment coefficients for the gust are shown. The function F in Equation (46) is minimized through the overall time, and the optimized incremental lift and moment coefficients are also shown. In the optimization, the magnitude of the lift coefficient was much greater than that of the pitching moment, and the function F represents essentially only the lift increment. Accordingly, to make both lift and moment terms of comparable size, the incremental lift and moment were scaled with respect to the peak lift and moment increments for the gust alone. These results are also shown in Figures 3 and 4. It can be seen that in the present simple analysis it is difficult for the two controls to alleviate both the lift and moment, although it is possible to control the lift itself quite well.

A similar series of data is shown in Figures 5 through 8 for a NACA 64A006 airfoil at $\alpha_m = 1.0$ degree and $M_\infty = 0.825$. Again, the agreement between the direct result and the present result is good. In the optimization cases, similar conditions to those noted for the previous example apply.

A third transonic case is shown in Figures 9 through 12. The airfoil is an MBB-A3 section at $\alpha_m = 1.5$ degrees and $M_\infty = 0.7$. The agreement between the direct result and the present result is good; the same general conclusions regarding optimization noted earlier apply.

The fact that the gust loading of the first transonic example can be alleviated more than the subsonic example would reinforce the suggestion made in section 8.

10. Possible Extensions of Work

The main advantage of the present technique is that the computational effort is minimal, thus allowing the use of an optimization routine to determine the best control movements. Provided the number of shock waves in the flow does not change, the method is very useful. If the number of shock waves does change during the unsteady motion, the present theory is invalid; however, it may be possible to extend the theory to treat this aspect. Such an extension for steady flow is given in Reference 13. There is no difference in principle in the indicial theory between two and three dimensions, and a logical extension of the present work would be to three-dimensional flows.

Several aspects of the existing two-dimensional procedure need improving. One aspect concerns the problems that can arise when the supersonic bubble is small and near the leading edge. The present method uses only one point straining (at the shock

wave). It has been found in earlier work on the steady flow problem that the points characterizing large gradients also need to be strained. Such a modification is a straightforward task. A second aspect is that the optimization code CONMIN may not be the best code to use; further study of the possibilities of using a different optimization code is desirable.

Because of the computational speed of the present method, it can be used to investigate different methods of gust alleviation, including radical concepts. The main restriction on the present work is that the aerodynamics of such devices must be capable of being modeled by potential theory. This restriction is because, at present, unsteady transonic flows are not routinely calculated by the Euler or Navier-Stokes equations. If such simulations were available, the indicial method would be applicable. It should be noted that a Navier-Stokes simulation is similar to experimental data in principle.

11. Conclusions

A method for predicting the gust loading on an airfoil moving at transonic speeds based on the indicial theory has been developed that is computationally efficient. The method allows easy incorporation of gust alleviation devices and, when linked to an optimization method, gives the best mode of operation of these control devices. The method should be applicable to three-dimensional flows where a considerable savings in computer resources over a direct simulation of the unsteady flow could be obtained. The method is semi-analytic in nature, which allows greater insight into methods of gust alleviation than can be obtained from a purely numerical study. Further study of the equations should lead to new ideas for alleviating the effect of gusts.

REFERENCES

1. Rizzetta, D. P. and Borland, C. J.: Numerical Solution of Three-Dimensional Unsteady Transonic Flow Over Wings Including Viscous Interaction. AIAA Paper 82-0352.
2. Ballhaus, W. F. and Goorjian, P.M.: Implicit Finite-Difference Computations of Unsteady Transonic Flows About Airfoils Including the Effect of Irregular Shock Motions. AIAA J., Vol. 15, No. 12, Dec. 1977, pp. 1728-1735.
3. Murman, E. M. and Cole, J. D.: Calculation of Plane Steady Transonic Flow. AIAA J., Vol. 9, No. 1, Jan. 1971, pp. 114-121.
4. Ballhaus, W. F. et al.: Improved Computational Treatment of Transonic Flow Past Swept Wings. Advances in Engineering Sciences, Vol. 4, NASA CP-2001, 1976, pp. 1311-1320.
5. Jameson, A. and Caughey, D.: A Finite Volume Method for Transonic Potential Flow Calculations. Proceedings of AIAA 3rd Computational Fluid Dynamics Conf., 1977.
6. Rizzetta, D. P. and Chin, W. C.: Effect of Frequency in Unsteady Transonic Flow. AIAA J., Vol. 17, No. 7, Jul. 1979, pp. 779-781.
7. Whitlow, W.: XTRAN2L - A Program for Solving the General Frequency Unsteady Transonic Small Disturbance Equation. NASA Tech. Memo 85223, 1983.
8. Ballhaus, W. F. and Goorjian, P. M.: Computation of Unsteady Transonic Flows by the Indicial Method. AIAA J., Vol. 16, No. 2, Feb. 1978, pp. 117-124.

REFERENCES (Cont.)

9. Nixon, D.: Notes on the Transonic Indicial Method. AIAA J., Vol. 16, No. 6, Jun. 1978, pp. 613-616.
10. Kerlick, G. D. and Nixon, D.: Calculation of Unsteady Transonic Pressure Distributions by the Indicial Method. App. Mech., Vol. 49, No. 2, Jun. 1982, pp. 273-278.
11. Ballhaus, W. F. et al.: Unsteady Force and Moment Alleviations in Transonic Flow in Unsteady Aerodynamics. AGARD CP-227, 1978.
12. McCroskey, W. J. and Goorjian, P. M.: Interactions of Airfoils with Gusts and Concentrated Vortices in Unsteady Transonic Flow. AIAA Paper 83-1691, Jul. 1983.
13. Nixon, D. and Kerlick, G. D.: Perturbations of a Transonic Flow with Vanishing Shock Waves. AIAA J., Vol. 23, No. 6, Jun. 1985, pp. 965-967.

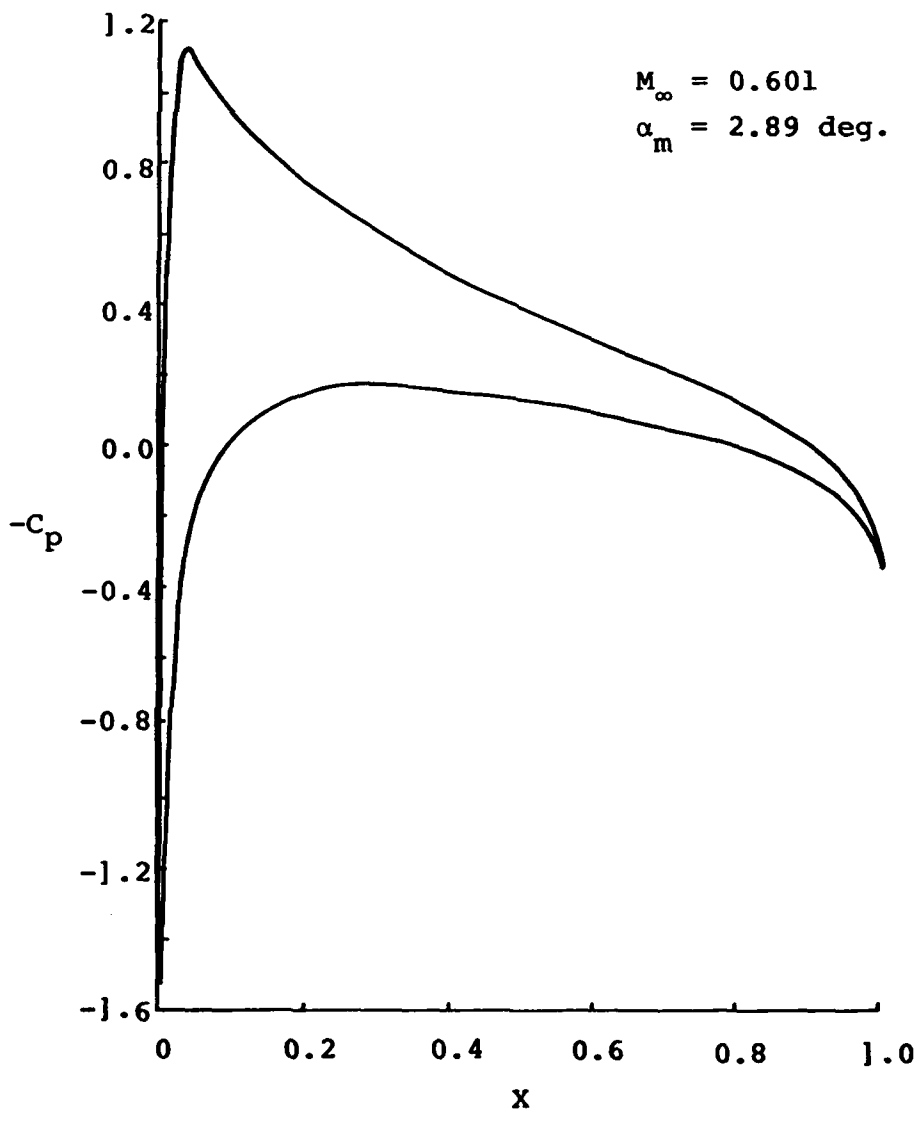


Figure 1. Steady state pressure distribution for a NACA 0012 airfoil.

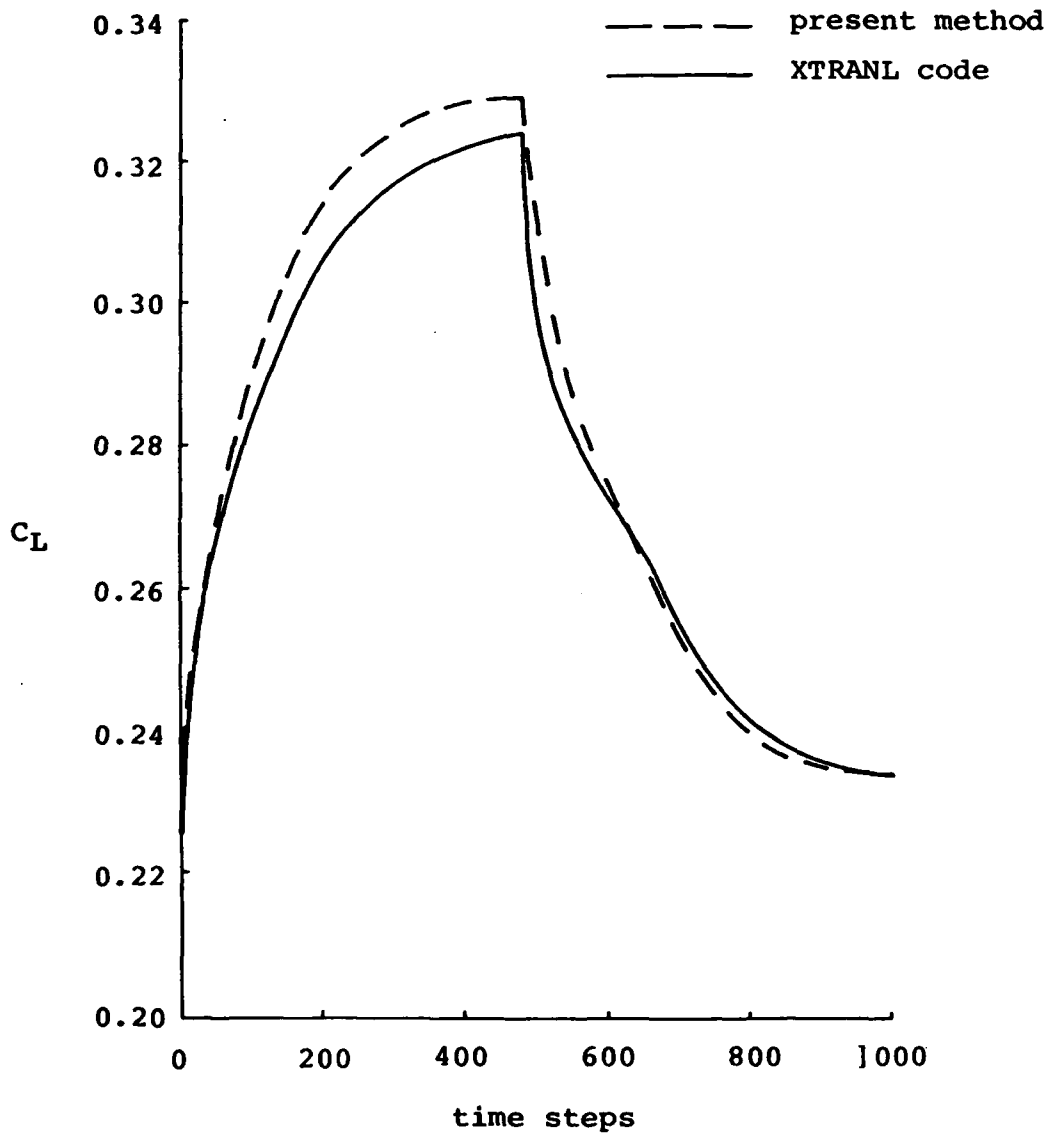


Figure 2. Test case comparison between present method and XTRANL for a NACA 0012 airfoil at $M_\infty = 0.601$ and $\alpha_m = 2.89$ degrees.

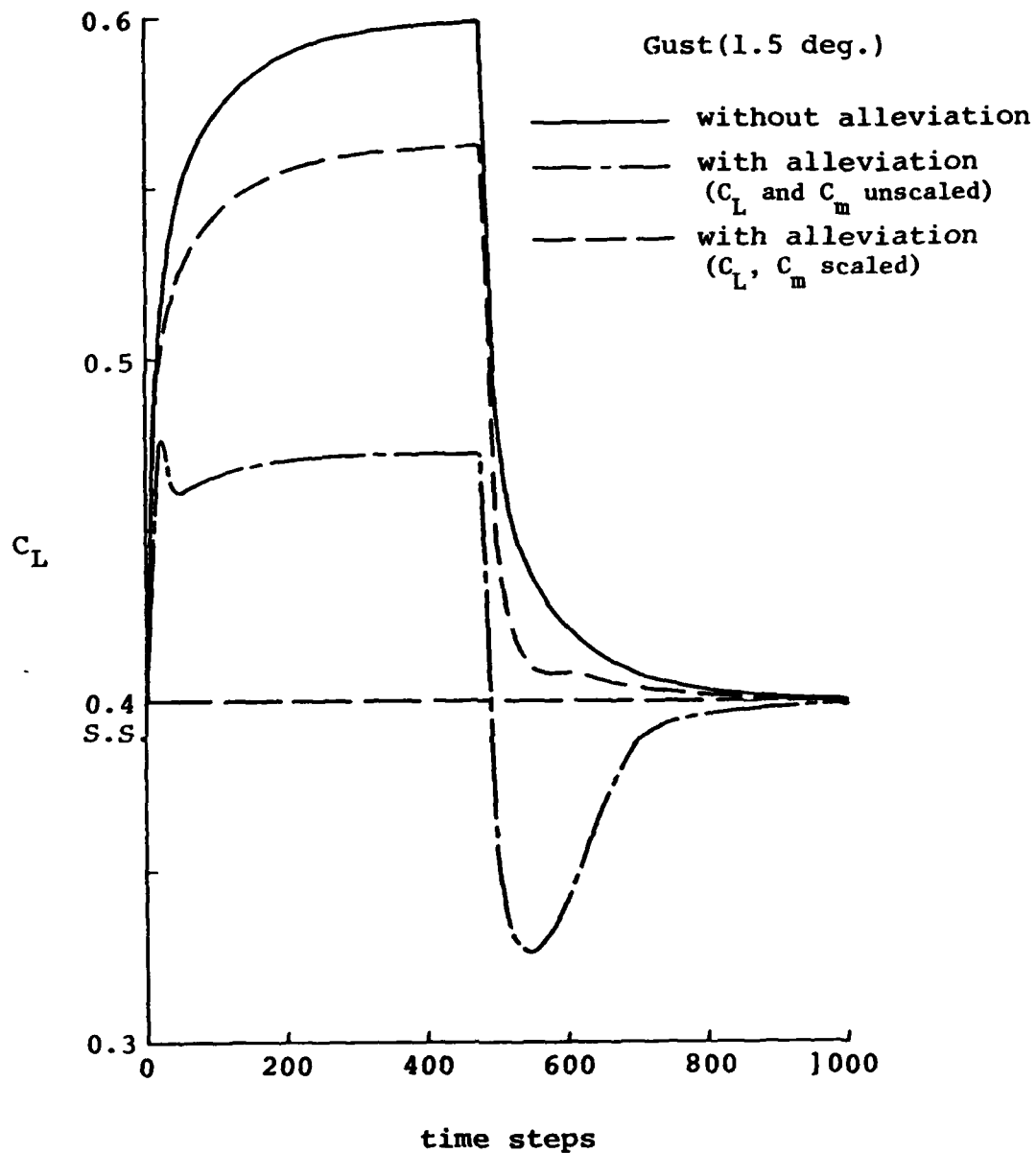


Figure 3. C_L comparison between gust with and without control surface deflection alleviation for a NACA 0012 airfoil at $M_\infty = 0.601$ and $\alpha_m = 2.89$ degrees.

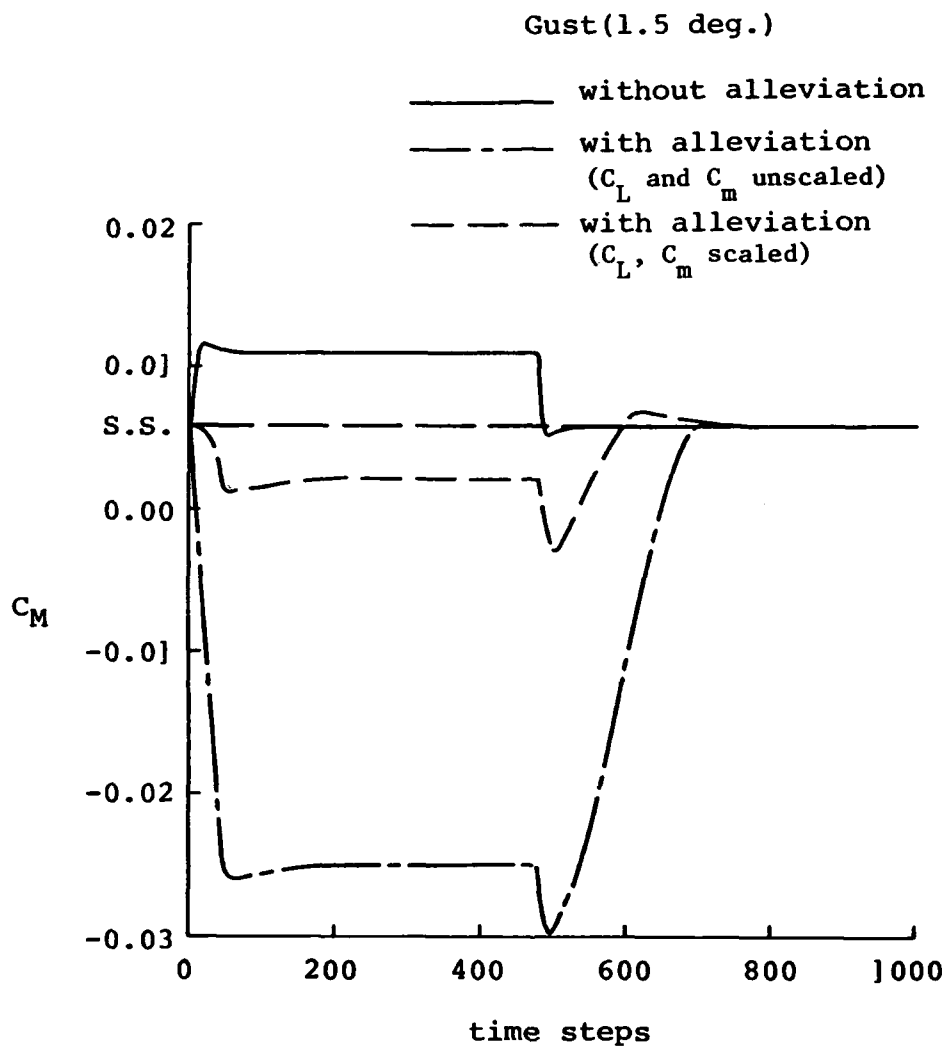


Figure 4. C_M comparison between gust with and without control surface deflection alleviation for a NACA 0012 airfoil at $M_\infty = 0.601$ and $\alpha_m = 2.89$ degrees.

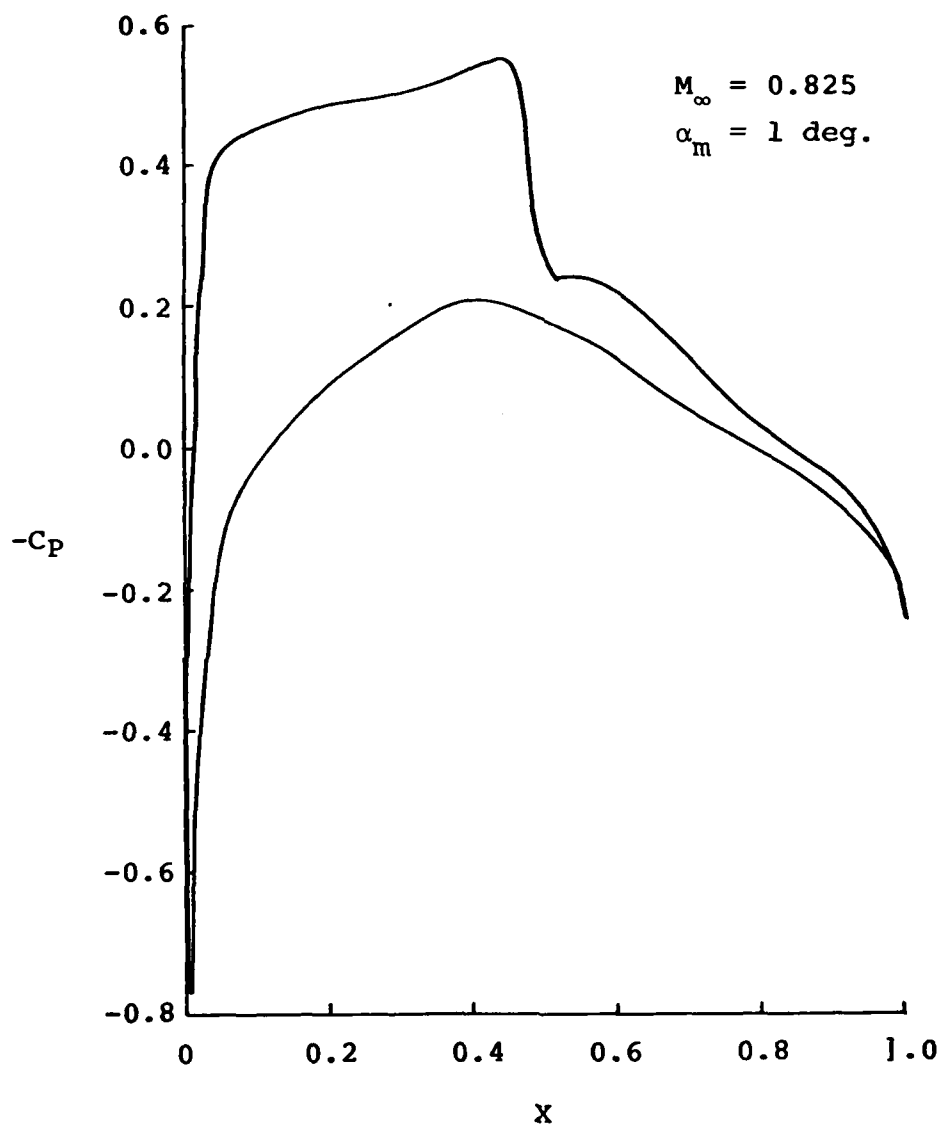


Figure 5. Steady state pressure distribution for a NACA 64A006 airfoil.

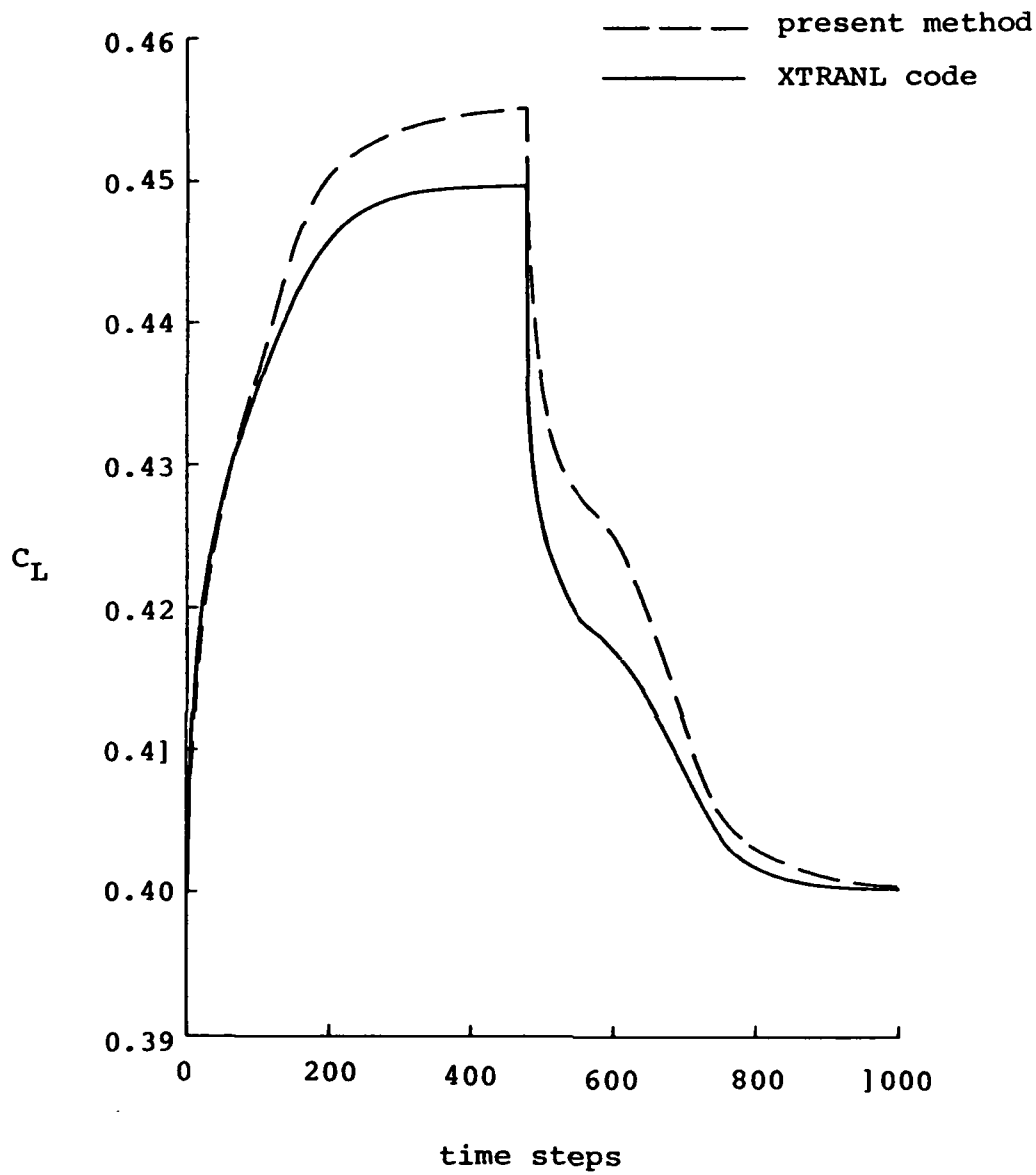


Figure 6. Test case comparison between present method and XTRANL code for a NACA 64A006 airfoil at $M_\infty = 0.825$ and $\alpha_m = 1$ degree.

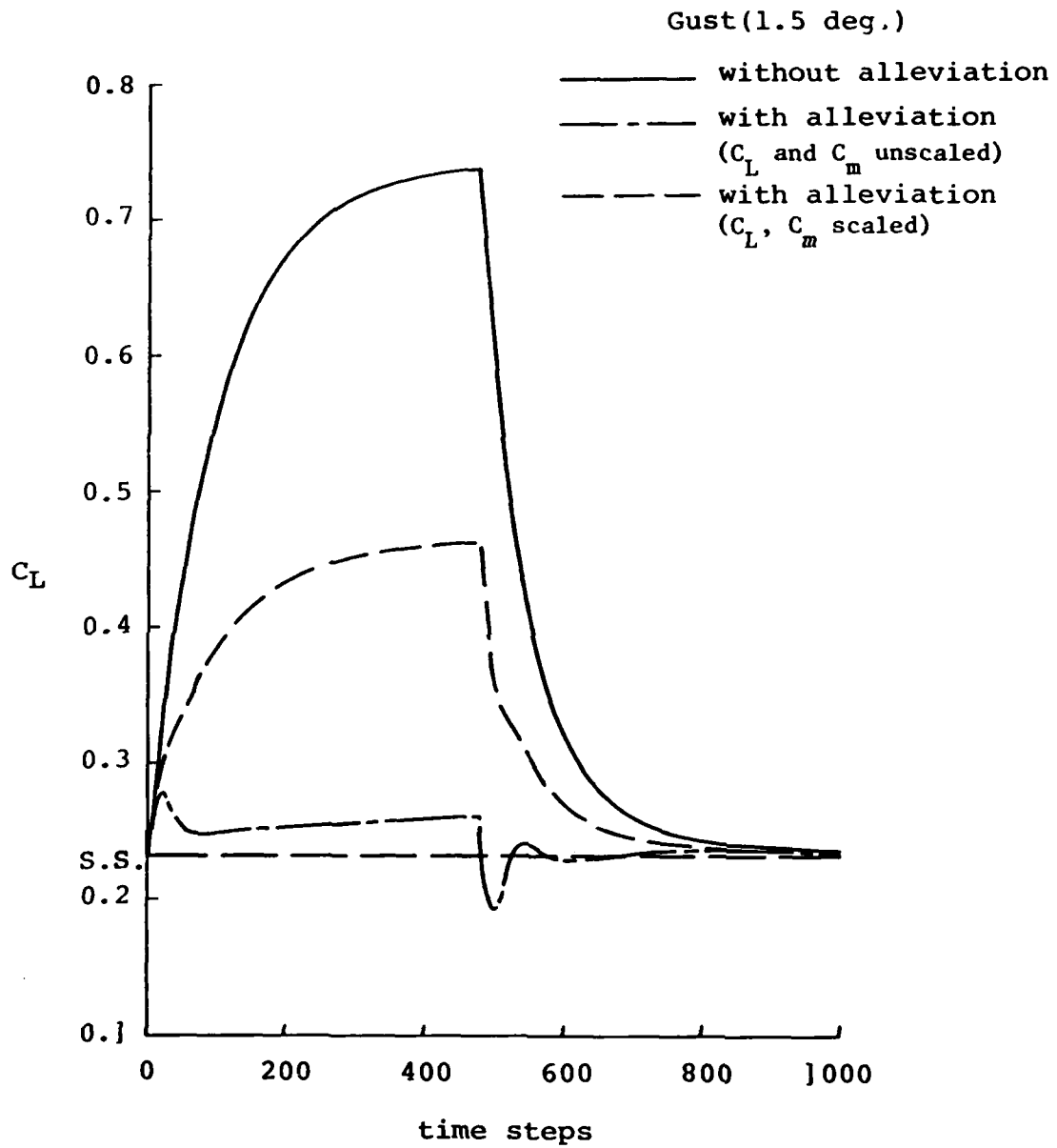


Figure 7. C_L comparison between gust with and without control surface deflection alleviation for a NACA 64A006 airfoil at $M_\infty = 0.825$ and $\alpha_m = 1$ degree.

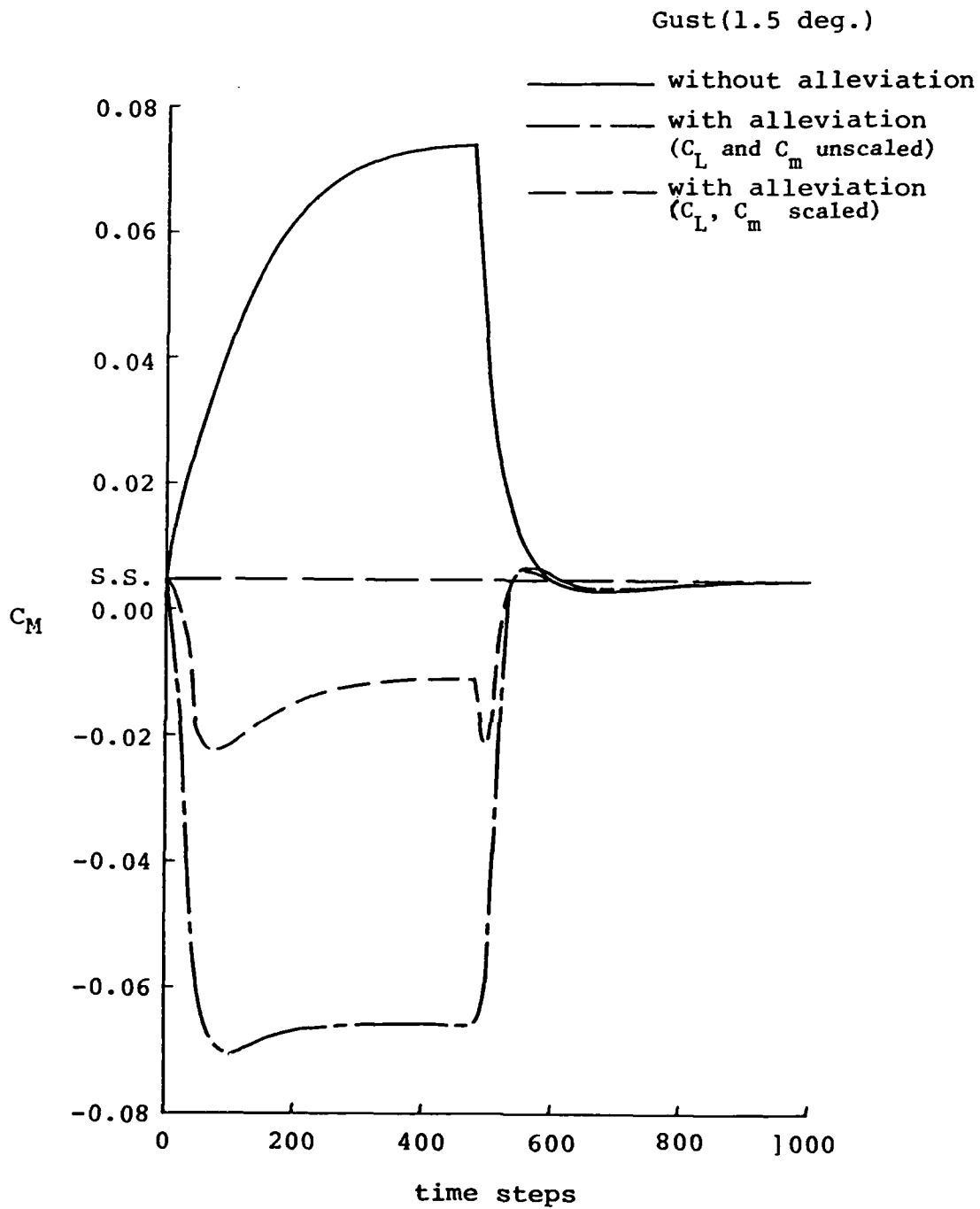


Figure 8. C_M comparison between gust with and without control surface deflection alleviation for a NACA 64A006 airfoil at $M_\infty = 0.825$ and $\alpha_m = 1$ degree.

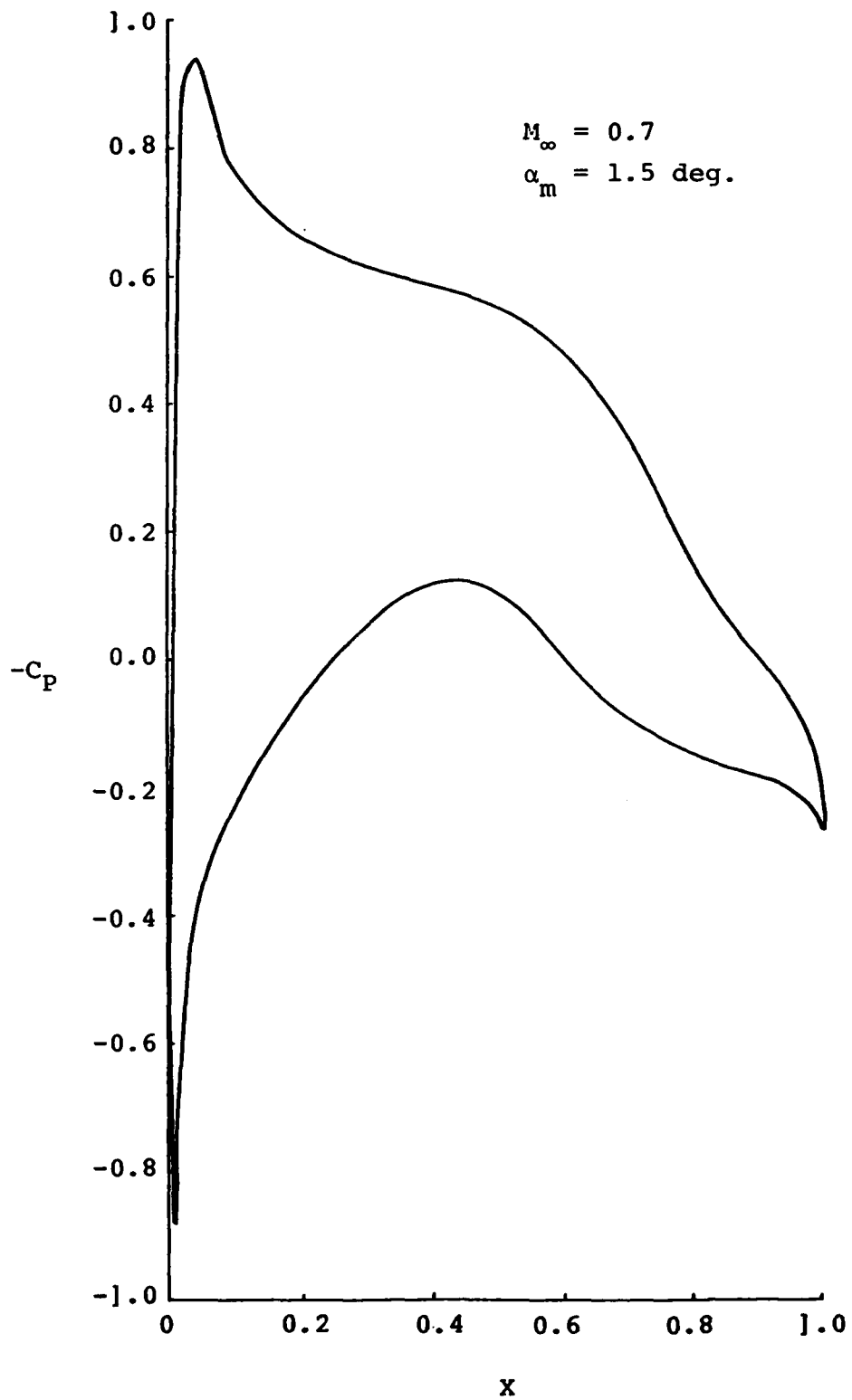


Figure 9. Steady state pressure distribution for an MBB-A3 airfoil.

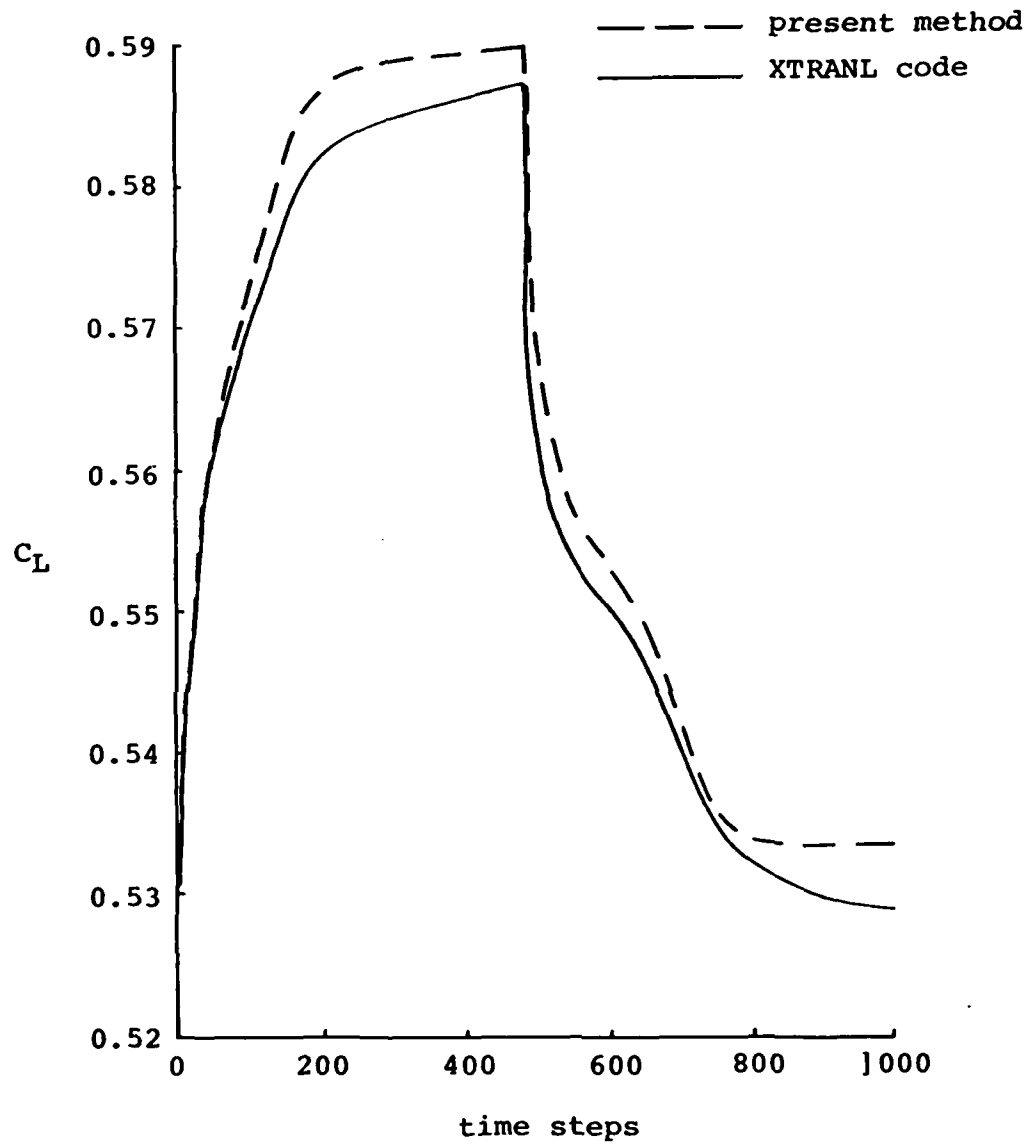


Figure 10. Test case comparison between present method and XTRANL code for an MBB-A3 airfoil at $M_\infty = 0.7$ and $\alpha_m = 1$ degree.

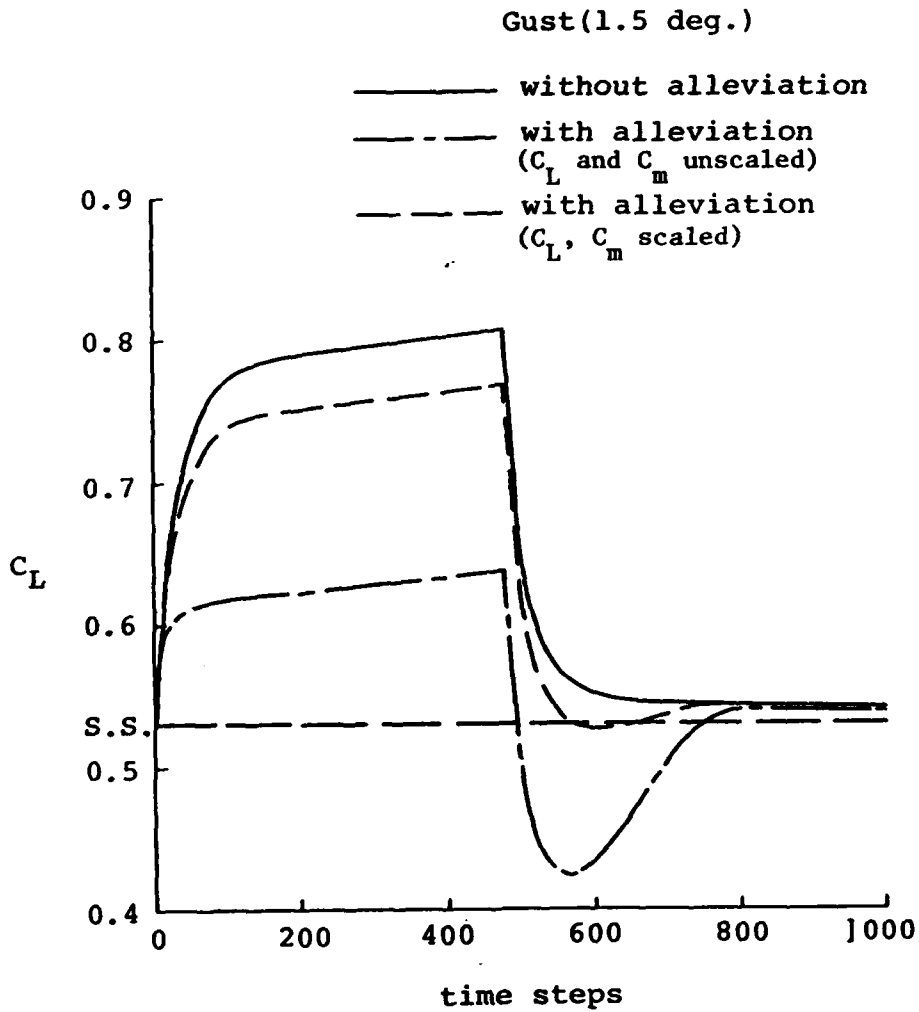


Figure 11. C_L comparison between gust with and without control surface deflection alleviation for an MBB-A3 airfoil at $M_\infty = 0.7$ and $\alpha_m = 1.5$ degrees.

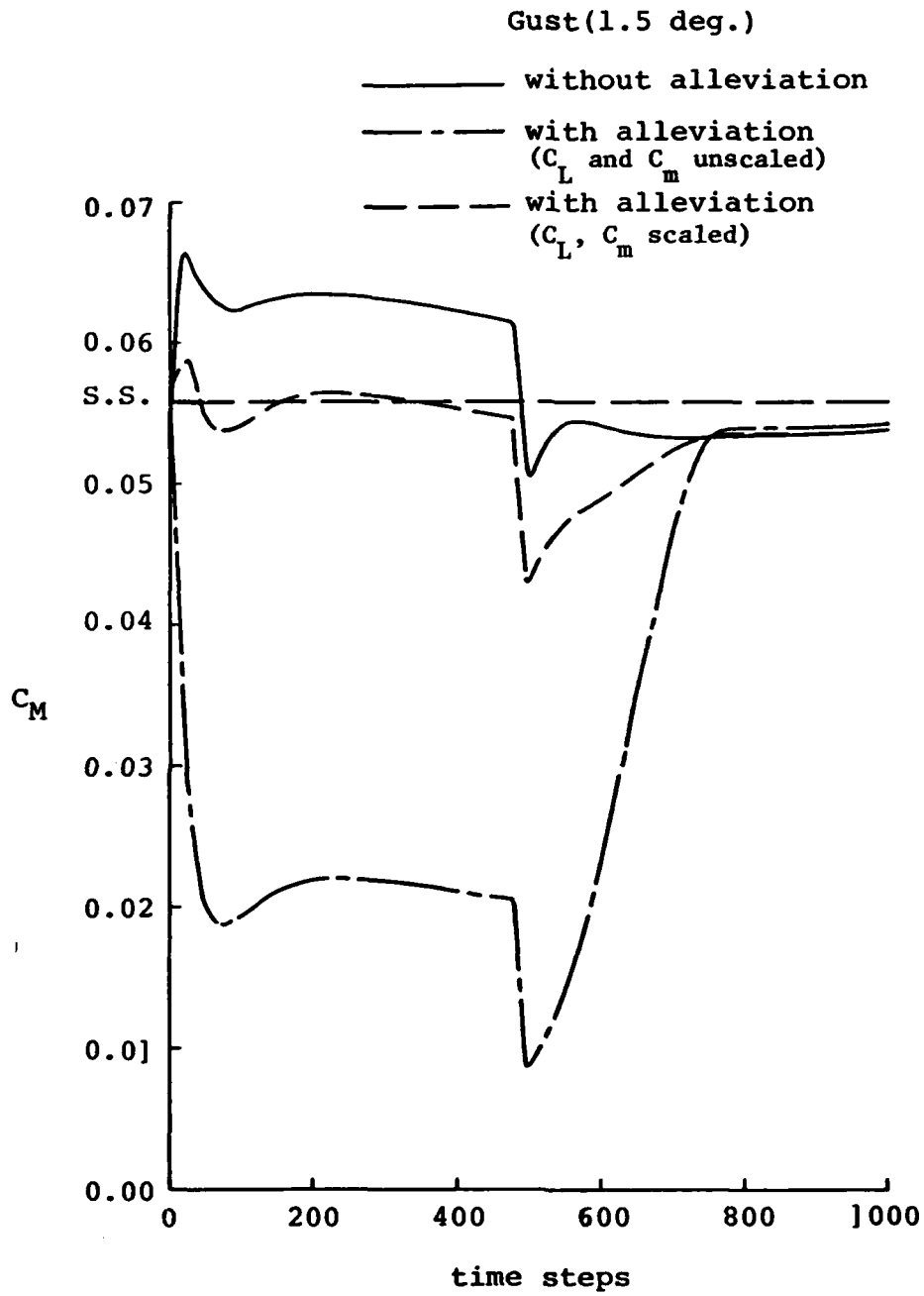


Figure 12. C_M comparison between gust with and without control surface deflection alleviation for an MBB-A3 airfoil at $M_\infty = 0.7$ and $\alpha_m = 1.5$ degrees.

END

DTIC

6-86